Optical Engineering

OpticalEngineering.SPIEDigitalLibrary.org

All-optical mitigation of amplitude and phase-shift drift noise in semiconductor optical amplifiers

Peterson Rocha
Cristiano M. Gallep
Evandro Conforti

SPIE.

All-optical mitigation of amplitude and phase-shift drift noise in semiconductor optical amplifiers

Peterson Rocha,[a] Cristiano M. Gallep,[b] and Evandro Conforti[a,*]
[a]University of Campinas, Faculty of Electrical and Computing Engineering-FEEC, Av. Albert Einstein 400, Campinas, SP 13083-970, Brazil
[b]University of Campinas, School of Technology, R. Paschoal Marmo 1888, Limeira, SP 13484-332, Brazil

Abstract. An all-optical scheme aimed at minimizing distortions induced by semiconductor optical amplifiers (SOAs) over modulated optical carriers is presented. The scheme employs an additional SOA properly biased to act as a saturated absorber, and thus counteract the distortions induced by the first amplifying device. The scheme here is demonstrated *in silico*, for 40 and 100 Gb/s (10 and 25 Gbaud, 16 QAM), with reasonable total gain (>20 dB) for symbol error rate below the forward error correction limit. [DOI: 10.1117/1.OE.54.10.106110]

Keywords: all-optical mitigation; phase noise; quadrature amplitude modulation systems; semiconductor optical amplifier.

Paper 150801 received Jun. 17, 2015; accepted for publication Sep. 24, 2015; published online Oct. 27, 2015.

1 Introduction

The increasing demand for bandwidth in telecommunication services keeps pushing the transmission rate growth in optical networks. The advent of multilevel modulation techniques increased spectral efficiency and postprocessing of impairments.[1] The most common modulation formats are the quadrature phase-shift keying (QPSK) and the M-ary quadrature amplitude modulation (M-QAM), already matured for commercial deployment.[2]

The semiconductor optical amplifier (SOA) is an attractive low-cost gain device for medium-range optical links, but in high-speed modulation formats with amplitude and phase-encoded optical carriers, the main SOA limitation is the small electronic carrier lifetime (around a nanosecond) producing pattern-dependent gain and severely degrading modulation symbols.[3]

Several techniques deliver regeneration of optical distortions, mainly for intensity-modulated carrier with direct detection.[4] In those simple systems, the optical carrier can be regenerated by its conversion to the electrical domain, followed by processing and conversion back to the optical domain.[5] Other approaches stabilize the signal amplitude using four-wave mixing in highly nonlinear fiber,[6] or self-pulse interactions in the nonlinear optical loop mirrors.[7] Other techniques enable reamplifying/reshaping (2R) with SOAs embedded in a Mach–Zehnder interferometer, where an additional optical source is needed,[8] or even by Sagnac interferometer, where wavelength conversion is also possible.[9]

For multilevel modulation formats, recent works are focused on digital approaches. The regeneration of QPSK signals, for example, can be implemented by using cross-phase modulation (XPM) in SOAs,[10] but with the need of an extra continuous wave (CW) laser. A similar approach using XPM and self-phase modulation (SPM) is based on nonlinear fibers.[11]

For 16-QAM signals, SPM in highly nonlinear fibers was used as well, enabling all-optical 2R regeneration by signal amplification/deamplification in the phase-sensitive amplifiers.[12] Many works propose to postcompensate the SOA impairments by digital backpropagation during the offline digital signal processing.[13–16]

In this work, we proposed a simple scheme for all-optical regeneration of optical signals with multilevel modulation when distorted by amplification in SOAs—a second SOA, properly biased below the transparency level in order to work as a nonlinear saturable absorber (SA), is used in the sequence of the first SOA amplifier device. In this way, the amplitude and phase noises are reduced, since the block amplifier-regenerative absorber composed of two SOAs works as an equalized amplifier. A similar technique was used previously to minimize amplitude distortions of rectangular pulses.[17] As demonstrated by simulations, the scheme enables the amplification of 16-QAM optical signals with small symbol distortions, operating below the forward error correction (FEC) limit for output powers up to 25 dBm and an overall gain of 20 dB.

Such a subsystem is a cheap option for signal amplification in medium-range networks (<20 km) and could be integrated in a single waveguide. This scheme can be optimized, depending on optical input power, by tuning the bias current of the second SOA.

Advanced modulation formats such as M-ary QAM encode a data signal in the amplitude and the phase of the optical electric field. Its complex vector E is coherently received and described by M points (symbols) in a complex constellation plane. The received E_r deviates by an error vector E_{err} from the ideal transmitted vector E_t. The error vector magnitude (EVM) is defined by a root mean square of the various E_{err} for N randomly transmitted symbols.[18,19] The bit error rate (BER) can be estimated from the measured EVM data:[20]

$$\mathrm{BER} \approx \frac{1-L^{-1}}{\log_2 L}\,\mathrm{erfc}\left[\frac{3\log_2 L}{(L^2-1)(k\mathrm{EVM}_m)^2\log_2 M}\right]^2, \qquad (1)$$

*Address all correspondence to: Evandro Conforti, E-mail: conforti@decom.fee.unicamp.br

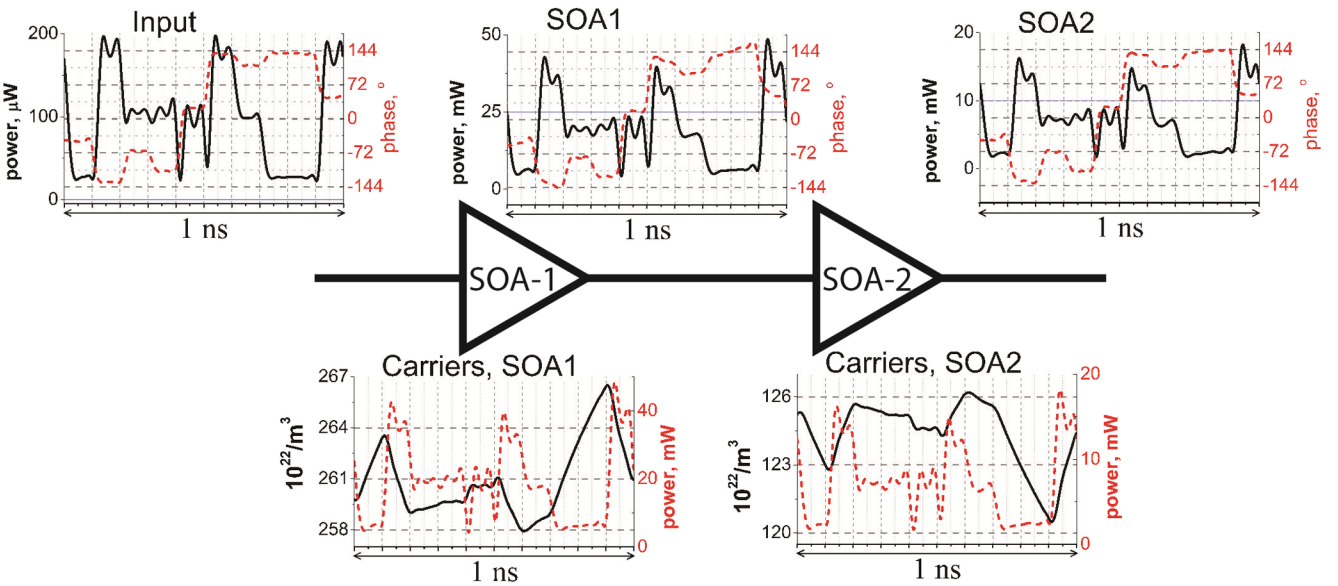

Fig. 1 Operation principle: amplitude- and phase-modulated optical signal (10 Gbaud, 16 QAM) entering semiconductor optical amplifier (SOA)-1 and leaving with distortions due to fluctuations in carrier density (i.e., in gain/phase); further entering SOA-2 and leaving with smaller distortions in amplitude and phase; note the inverted variation in carrier density for each device.

where L denotes the number of signal levels in each dimension (e.g., $L_{16\text{QAM}} = 4$), and $\log_2 M$ is the number of bits encoded into each symbol. The conversion factor k converts the normalized EVM by using the outermost constellation point to the EVM defined by the average power.

2 Distortion and Regeneration of Multilevel Optical Signals in Semiconductor Optical Amplifiers

The signal distortion inherent in optical amplification in SOAs is mainly due to its small carrier lifetime (~1 ns) in such a way that variations in the input optical power lead to electronic carrier fluctuations within a time slot enough to modify the gain and phase delay, which appear as amplitude and phase noise over the output signal.[21] The same process can be used in a reverse mode in a second SOA, with a small or even no current injection ($I_{\text{bias}} \sim 0$), to operate as a saturated absorber capable of minimizing the symbol distortions induced by the first SOA. By absorbing high-input power peaks, and inducing opposite refractive index changes to counteract phase-distortions, the SA can equalize the main distortions induced by SOA amplification at first. Even though the use of a second SOA to act as an SA could lead to a worse optical signal-to-noise ratio (OSNR) at the output carrier, since a small electronic population inversion is used in this case, the fluctuations in amplitude and phase can be minimized by the nonlinear absorption process.

This process is illustrated in Fig. 1, where an optical carrier with modulations in amplitude and phase (16 QAM, 10 Gbaud) enters SOA-1; this first device is fed by a high bias current promoting enough electronic carrier population for a high optical gain (>25 dB). When the optical input power increases—as in the bit at $100 < \Delta t < 200$ ps—the signal initially receives a high optical gain by stimulated emission, thus consuming the electronic carrier density that is quickly depleted by a few percent, but is still enough to infringe a lower optical gain in the rest of the optical symbol. Because the phase shift during amplification is carrier-density-dependent,[21,22] the fluctuations of the carrier density also deteriorate the output phase stability, distorting the beginning of the symbol by tens of degrees ($100 < \Delta t < 150$ ps). When the input power decreases—as in the $700 < \Delta t < 900$ ps—the lowest absolute carrier consumption enables the carrier density to increase by current injection, thus the last part of the bit slot is distorted similarly in both amplitude and in phase, as we described. The high optical power signal that leaves the first SOA then passes through a second SOA (SOA-2), which is poorly biased ($I_{\text{bias}} \sim 0$ mA) and acts as an absorber. Therefore, the carrier density is fed mainly by optical absorption of the input signal, with the carrier density behaving in opposition time to that occurring in the first SOA. For SOA-2, high optical input powers lead to higher electronic carrier density, which leads to less attenuation, and vice-versa for small optical powers. At the same time, the induced phase-shift at SOA-2 is opposite to that of SOA-1, and the output signal has a reduction in the fluctuations of phase and/or amplitude of the output signal's symbols.

Thus, if after the first SOA, the amplifying one, a second "dark" SOA, is conveniently biased, it acts as a nonlinear absorber, and the total result of SOA-1 + SOA-2 is an equalized amplifier. For each input power, an optimum $I_{\text{bias}} > 0$ can be found for SOA-2 in order to provide the best phase and amplitude regeneration.

3 Simulations and Results

Figure 2 shows the block diagram for the simulated scheme, with the "quasi"-linear amplifier composed of two concatenated, discrete SOAs, but that could also be implemented by an integrated two-section SOA. The device parameters are shown in Table 1, and the complete simulation scheme is presented in the Appendix.

The performance for the equalized amplifier scheme was studied for an optical link with a single optical carrier (single channel) and with five simultaneous carriers (multichannel)

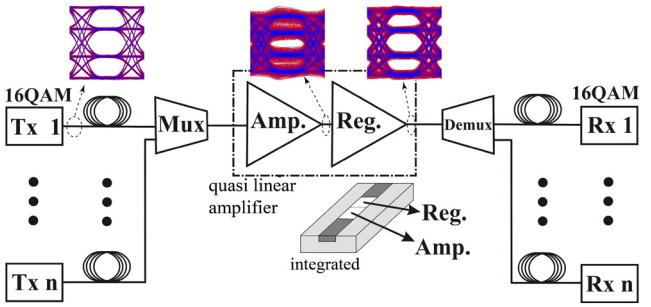

Fig. 2 Multichannel, 16-QAM optical system employing the equalized amplifier—two concatenated SOAs or an integrated SOA with two sections. In detail from left to right, the eye-diagrams after Tx (back-to-back), and after SOA-1 and SOA-2.

Table 1 Parameters for the semiconductor optical amplifier, bulk-like active cavity.[23]

Parameter	Value
Section length	0.65 mm
Active region width	33×10^{-4} mm
Active region thickness	15×10^{-5} mm
Effective index	2.9
Group index	3.75
Internal loss	1500 m^{-1}
Confinement factor	0.5
Optical coupling efficiency	1.0
Interface reflection coefficient	5×10^{-5}
Interface reflection phase left	180.0 0.0
Effective mode area	10^{-12} m^2
Gain shape model	Flat
Gain model	Linear
Gain coefficient linear	1.75×10^{-23} m^2
Nonlinear gain coefficient	0.5×10^{-23} m^3
Nonlinear gain time constant	500×10^{-15} s
Carrier density transparency	1.5×10^{24} m^{-3}
Linear recombination	1.5×10^{8} s^{-1}
Bimolecular recombination	2.5×10^{-17} m^3 s^{-1}
Auger recombination	9.4×10^{-41} m^6 s^{-1}
Initial carrier density	0.8×10^{24} m^{-3}

modulated with 16 QAM. The single-channel system was tested using two discrete SOAs—0.65-mm-long each; and using a single, integrated two-section-SOA with the same dimensions, for modulation rates of 10 and 25 Gbaud (40 and 100 Gb/s, pseudo-random binary sequence (PRBS) $2^{13} - 1$), with an input optical power from −20 to −10 dBm in the C-band. A 16-QAM-Tx launches an optical carrier (0 dBm) to propagate in a fiber link before reaching the amplifier scheme. The bias current for SOA-1 was fixed in 150 mA; for SOA-2, the bias varied from 0 to 20 mA (stronger to weaker input powers) to optimize each case of data rate/input power. The symbols' constellation was evaluated by its EVM at the Tx (back-to-back) after the first and the second SOAs.

Figure 3 shows the EVM for these cases for both the discrete and the integrated device schemes. The input constellation had a small noise added in order to have an initial EVM <6% (b-t-b). After SOA-1, the constellations appear distorted, with more pronounced rotation for high input powers as expected.[21,22] Even for moderate inputs powers (less than −15 dBm), the signal amplified by a single SOA exceeds the FEC limit (EVM < 12%). For the 10-Gbaud case, the second, (SA)-SOA was able to correct the constellation rotation for all cases, always keeping the EVM always below the FEC limit for both the discrete and the integrated devices. For the worst case (input power = −10 dBm), the distortion is reduced from 24% to 12%. The best case (−20 dBm input) presents an output constellation similar to that of the back-to-back case.

For the 25-Gbaud case, with shorter bit slots, the SOA gain presents lower dynamic variations, and the signal is not so deteriorated by SOA-1 as for the 10-Gbaud case. After SOA-2, the constellation is high regenerated as in the previous case, but not for the integrated device and small input powers (−20 dBm). This can be explained by the particular model used here to simulate the integrated SOA, which has a single active cavity fed by two bias gates—even when not feeding the second bias, the electrical current sent to the first bias gate diffuses through the semiconductor guide and populates the second section. For the worst case (−10 dBm input), the output EVM can be improved from 18% to 12%. If two independent SOAs are used in the integration scheme, instead of a single device with two bias sections, a behavior like that of the discrete scheme is expected.

To test the amplifier scheme performance in multichannels optical links, an optical system with five channels was simulated in similar conditions. The five carriers were spaced by 100 GHz in the C band, 0-dBm power each. EVM results are shown in Fig. 4 for the integrated SOAs' configuration. Regarding 10-Gbaud carriers, the scheme is able to amplify all channels without a stronger distortion for all input powers up to −10 dBm. In the worst case (−10 dBm), the distortion is reduced from 15.5% to 11.5%, which is below the actual FEC limits. For 25 Gbaud, all EVM curves are similar to each other. For a small input power (−20 dBm), the amplified spontaneous emission noise of the first SOA preponderates and causes the worst EVM in this case. For a −10 dBm input power, the signal degradation induced by SOA-1 is improved after SOA-2, with the EVM reduced from 13% to 10.5%, which is again below the FEC limit.

In both cases of Fig. 4, the constellations are less distorted after SOA-1 than that for the single-channel configuration. This happens because for a multichannel link, the overall input power is the sum of the n channels, with intensity fluctuations minimized. Therefore, SOA-1 operates in a gain-clamped condition, with the total optical signal helping to

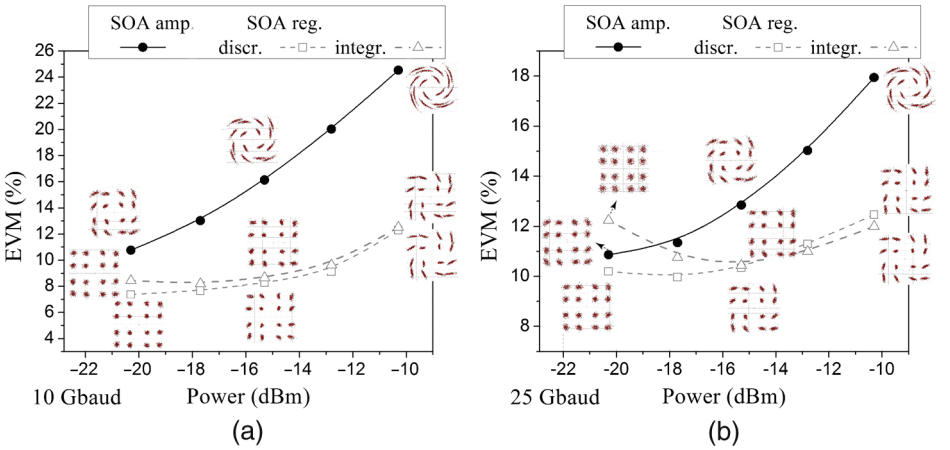

Fig. 3 Error vector magnitude (EVM) versus optical input power in the equalized amplifier, for a single-channel system at (a) 10 Gbaud and (b) 25 Gbaud, after SOA-1 and SOA-2, in discrete and integrated configurations; note examples of the signal constellation for small (−20.2 dBm), moderate (−15.5 dBm), and highly moderate (−10.2 dBm) input powers for each case.

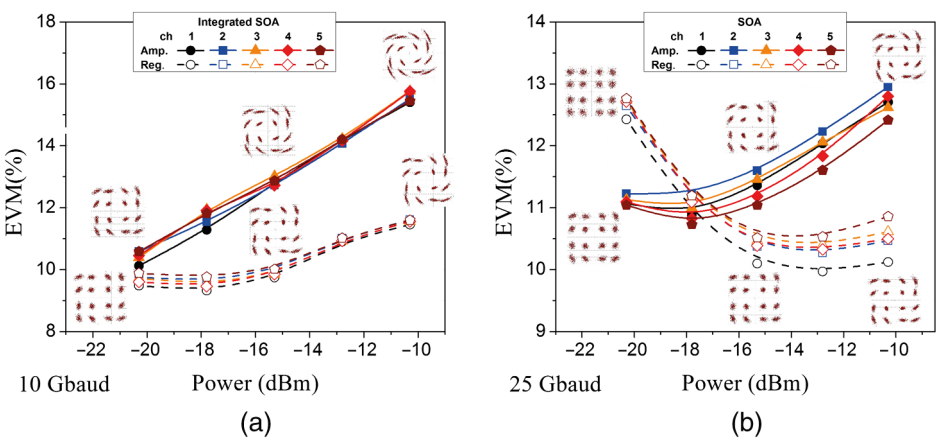

Fig. 4 EVM versus optical input power in the equalized amplifier, for the multichannel system in (a) 10 Gbaud and (b) 25 Gbaud, after SOA-1 and SOA-2 (reg.) in integrated configuration; note examples of signal constellation for small (−20.2 dBm), moderate (−15.5 dBm), and highly moderate (−10.2 dBm) input powers for each case.

equalize the carrier density in time, thus the overall gain fluctuates less for all of the channels.

4 Conclusion

An equalized amplifier formed of two concatenated SOAs—one amplifying and the other slightly absorbing the optical signal—was presented and numerically studied for 16-QAM optical carriers, enabling operation for single channel and multichannel optical links at 10 and 25 Gbaud, for input powers from −20 to −10 dBm. Higher optical input powers induce a too strong distortion at the amplifying device and further regeneration at the second device is not effective enough to operate below the FEC limits, narrowing the range of operation in relation to the input power. Since just a few dB (3 to 6) of absorbed optical power at the second device is the price to be paid for all-optical mitigation of SOA-induced distortions, we believe it can be successfully used for middle-range optical links, even in modern flex-grid/flex format networks, in a scheme transparent to modulation format and symbol rate.

In practice, it could be hard to optimize the I_{bias} for a commercial SOA designed to be a good amplifier to act as a good SA; the best SA point could be easily overlapped to a very bad noise-figure operation point, since a small electronic carrier population inversion is used in such a case.

But other devices have already been successfully demonstrated for such a purpose, when nonlinear phase shifts are dependent on the optical input power on ion-implanted waveguides.[24–26] Reduction of noise figure was also demonstrated for a multisection, properly biased SOA device.[27] Another option to implement the SA would be a semiconductor cavity with vertical arrangements, as has already been used to compensate for SPM impairments;[28–30] in these devices, the changes in refractive index also depend on the optical intensity, and this is optimized by a proper resonant cavity.

Appendix: Simulations of the 16-QAM Optical Signal (VPItransmissionMaker™)

Two transmission rates were used to evaluate the performance of the two optical systems, 10 and 25 Gbaud. A CW laser of 0-dBm power and 10-kHz linewidth was used as an optical carrier (1550 nm). PRBS ($2^{13}-1$) is used to modulate the channel and to calculate the EVM.

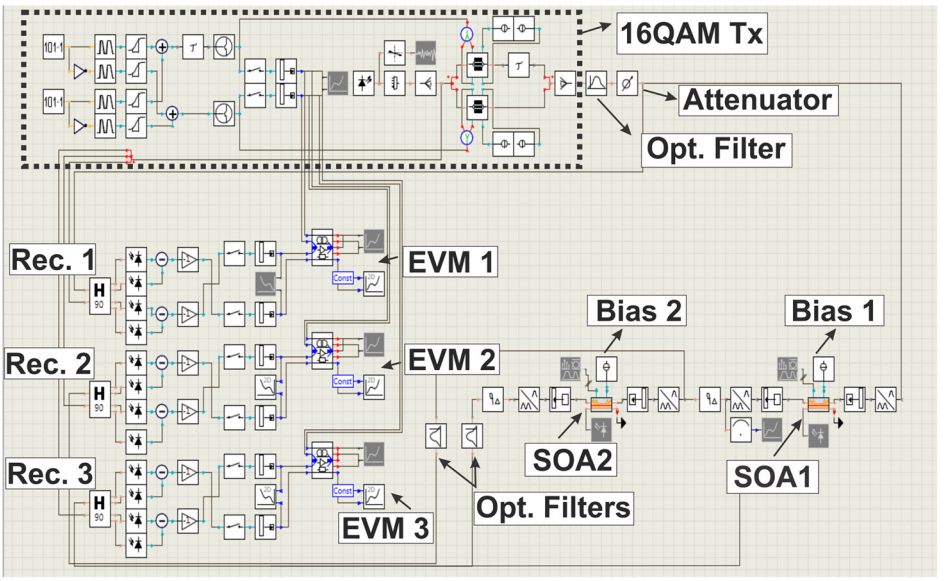

Fig. 5 Optical system, 16-QAM single channel, processed by two discrete SOAs. SOA1 with fixed bias of 150 mA; SOA2 (SA) with a few mA variable bias to achieve the lower EVM.[23]

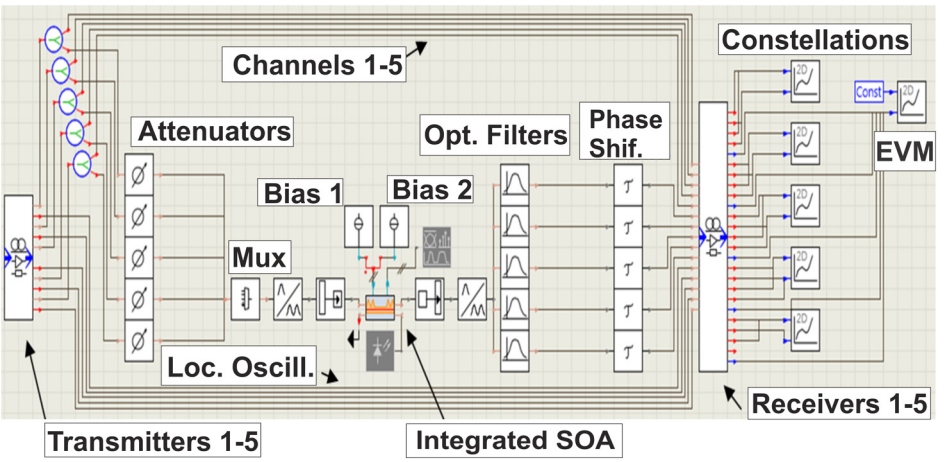

Fig. 6 Optical system, 16-QAM multichannel, processed by two-section integrated SOA.[23]

For a single-channel system (Fig. 5), Gaussian optical filters (50 GHz) were used for the Tx and Rx sites. The Rec. 1 corresponds to the b-t-b link; Rec. 2 to a single SOA system; and Rec. 3 to a dual device (SOA1 + SOA2) system.

Each receiver is formed by a 90 deg hybrid with balanced photodetectors and coherent homodyne reception.

All EVMs in both environments are obtained from the normalizations of the generated electric constellation and the received constellation. Attenuators are used in both environments to ensure optical input powers of −20.2, −17.8, −15.5, −12.8, and −10.2 dB in the SOA.

For the multichannel system (Fig. 6), the Tx comprises five multiplexed optical channels spaced by 100 GHz, with each one as the single channel of Fig. 5. The filters of the Rx subsystem were also used. Phase shifters are needed to synchronize all the received channels and enable EVM calculation.

Acknowledgments

The authors would like to thank CAPES (Coordination of Improvement of Higher Education Personnel), CNPq (National Council of Scientific and Technological Development), Espaço da Escrita-Coordenadoria Geralda Universidade-UNICAMP-for the language services provided and FAPESP (Foundation for Research Support of the State of São Paulo) (FAPESP/Padtec #2007/56024-4; #2015/50063-4), and INCT Fotonicom, (CNPQ 574017/2008-9) projects for partial financial support.

References

1. R. Essiambre and R. W. Thach, "Capacity trends and limits of optical communication networks," *Proc. IEEE* **100**, 1035 (2012).
2. J. D. Reis et al., "Bidirectional coherent WDM-PON performance with real-time Nyquist 16QAM transmitter," in *Optical Fiber Communication Conf., OSA Technical Digest (Online)*, Optical Society of America, Washington, DC (2015) paper Th3I.5.
3. R. Bonk et al., "Impact of alpha-factor on SOA dynamic range for 20 dBd BPSK, QPSK and 16-QAM signals," in *Optical Fiber Communication Conf. and Exposition and the National Fiber Opt. Engineers Conf.* (2011).
4. J. C. Simon et al., "All-optical regeneration," in *European Conf. on Optical Communication*, Vol. 1, pp. 467 (1998).
5. G. Agrawal, *Fiber-Optics Communication Systems*, 3rd ed., John Wiley & Sons, Inc., New York (2002).

6. M. Matsumoto and Y. Morioka, "Regeneration of RZ-DPSK signals by fiber-based all-optical regenerators," *IEEE Photonics Technol. Lett.* **17**, 1055 (2005).
7. V. Roncin et al., *SOA-NOLM in Reflective Configuration for Optical Regeneration in High Bit Rate Transmission System*," Cornell University Library, Ithaca, New York (2007).
8. L. Xi, Y. Ma, and L. Sun, "Regeneration of DQPSK signals using semiconductor optical amplifier-based phase regenerator," in *Int. Conf. on Advanced Infocom Technology*, pp. 1 (2011).
9. G. Gavioli and P. Bayvel, "Novel 3R regenerator based on polarization switching in a semiconductor optical amplifier-assisted fiber Sagnac interferometer," *IEEE Photonics Technol. Lett.* **15**, 1261 (2003).
10. Y. Zhan et al., "All-optical QPSK signal regeneration based on XPM in semiconductor optical amplifier," in *Communications and Photonics Conf.*, pp. 1 (2012).
11. M. Matsumoto, "All-optical DQPSK signal regeneration using 2R amplitude regenerators," *Opt. Express* **18**, 10 (2010).
12. L. Li and M. Vasilyev, "All-optical 2R regenerator of 16-QAM signals," *Proc. SPIE* **9009**, 900908 (2014).
13. X. Li and G. Li, "Joint fiber and SOA impairment compensation using digital backward propagation," *IEEE Photonics J.* **2**, 753 (2010).
14. S. Amiralizadeh, A. T. Nguyen, and L. A. Rusch, "Error vector magnitude based parameter estimation for digital filter back-propagation mitigating SOA distortions in 16-QAM," *Opt. Express* **21**, 20376 (2013).
15. A. Ghazisaeidi and L. A. Rusch, "Low complexity digital back-propagation for SOA," *IEEE Photonics Conf.*, pp. 686 (2011).
16. S. Amiralizadeh et al., "Experimental validation of digital filter back-propagation to suppress SOA-induced non linearities in 16-QAM," in *Optical Fiber Communication Conf. and Exposition and the National Fiber Optical Engineering Conf.* (2013).
17. K. Inoue, "Technique to compensate waveform distortion in a gain-saturated semiconductor optical amplifier using a semiconductor saturable absorber," *Electron. Lett.* **34**, 376–378 (1998).
18. R. Schmogrow et al., "Error vector magnitude as a permormance mesasure for advanced modulation formats," *IEEE Photonics Technol. Lett.* **24**, 61–63 (2012).
19. B. Nebendahl et al., "Quality metrics in optical modulation analysis: EVM and its relation to Q-factor, OSNR, and BER," in *Communications and Photonics Conf.*, pp. 1–3 (2012).
20. R. Schmogrow et al., "512QAM Nyquist sinc-pulse transmission at 54 Gbit/s in an optical bandwidth of 3 GHz," *Opt. Express* **20**, 6439–6447 (2012).
21. G. P. Agrawal and N. A Olsson, "Self-phase modulation and spectral broadening of optical pulses in semiconductor optical amplifier," *IEEE J. Quantum Electron.* **25**, 2297 (1989).
22. J. Wang et al., "Temporal dynamics of the alpha factor in semiconductor optical amplifiers," *J. Lightwave Technol.* **25**, 891 (2007).
23. VPItransmissionMaker™, www.vpiphotonics.com
24. Z. Bakonyi et al., "In-line saturable absorber in transmission systems with cascaded semiconductor optical amplifiers," *IEEE Photonics Technol. Lett.* **12**, 570–572 (2000).
25. Z. Bakonyi et al., "Noise suppression by saturable absorber in transmission systems with semiconductor optical amplifiers," in *Conf. on Lasers and Electro-Optics*, pp. 329–330 (2000).
26. M. Pantouvaki et al., "10 Gb/s noise suppression using an ion implanted waveguide saturable absorber," in *Conf. on Lasers and Electro-Optics/Quantum Electronics and Laser Science Conf.*, pp. 1–2 (2006).
27. K. Carney et al., "3.8 dB noise figure in bulk semiconductor optical amplifier," in *Conf. on Lasers and Eletro-Optics Pacific Rim*, pp. 1–2 (2013).
28. S. Suda et al., "High speed response of nonlinear optical phase-shifter based on vertical micro-cavity saturable absorber," *IEICE Electron. Express* **5**, 131–135 (2008).
29. S. Suda et al., "Optical nonlinear phase shifter using vertical micro-cavity with saturable absorber," in *Conf. on Lasers and Eletro-Optics/Quantum Eletronics and Laser Science Conf.*, pp. 1–2 (2006).
30. R. Pradhan and S. Saha, "Reflective vertical cavity quantum-well saturable absorber as an all-optical nonlinear phase-shifting element," *J. Opt. Soc. Am. B* **31**, 2956–2964 (2014).

Biographies for the authors are not available.